Single-atom engineering goldene for highly efficient and selective electroreduction of nitrate to ammonia

Zishan Xiong[a], Song Lu[a]*, Jiaqi Fan[a], Tiancun Liu[a]*, Qing Li[b], Yong Wu[c], Zhixin Yu[a]

[a]Institute of New Energy, School of Chemistry and Chemical Engineering, Shaoxing University, Shaoxing 312000, China.

[b]Department of Machine Learning, Mohamed bin Zayed University of Artificial Intelligence, Masdar 999041, Abu Dhabi.

[c]School of Chemistry, Dalian University of Technology, Dalian 116024, China.

Computational details

The adsorption free energy of NO_3^- adsorption on TM@goldene is calculated via the following equation[1]:

$$\Delta G_{*NO3} = G_{*NO3} - G_{*} - G_{*HNO3(g)} + 1/2G_{H2(g)} + \Delta G_{correct}$$

where G_{*NO3}, G_{*}, $G_{*HNO3(g)}$, and $G_{H2(g)}$ denote the Gibbs free energy of NO_3^- adsorbed on TM@goldene, clean TM@goldene, gaseous HNO_3 and H_2, respectively. $\Delta G_{correct}$ is the correction for NO_3^- adsorption energy, which is set to 0.392 eV[2].

To investigate the stability of vacancy-defect in goldene, the formation energy of Au vacancy is calculated by following equation:

$$E_f\,(V_{Au}) = E(V\text{-}Au) - n \times E_{Au}$$

where E(V-Au), n and E_{Au} are the total energy of defective goldene, the number of Au atoms and energy of each Au atom in a pristine golden, respectively.

To evaluate the thermodynamic stability of TM on vacancy-defected goldene, the formation energy (E_f) is calculated by the equation below:

$$E_f\,(TM@goldene) = E(TM@goldene) - E(TM) - E(vacancy\text{-}defected\ goldene)$$

Where E(TM@goldene), E(TM), E(vacancy-defected goldene) are the total energies of TM@goldene, single TM atom, and vacancy-defected goldene.

In addition, the electrochemical dissolution potential (U_{diss}) is also calculated to examine the electrochemical stability of the TM@goldene, which is given as follows[3]:

$$U_{diss} = U^0_{diss} - E_f\,(TM@goldene)/n$$

where U^0_{diss} and n are the standard dissolution potential of the TM and the number of electrons involved in dissolution.

Table S1. The lattice parameter (a, Å), the TM-Au bond lengths ($d_{TM\text{-}Au}$, Å), the formation energies (E_f, eV), the dissolution potential (U_{diss}, V) of TM@goldene, the Gibbs free energy change for NO_3^- with two-O model, NO_3^- with single-O model, H, and N_2 adsorption.

TM	a	$d_{TM\text{-}Au}$	E_f	U_{diss}	G_{*NO3} (two-O)	G_{*NO3}(single-O)	G_{*H}	G_{*N2}
Sc	16.38	2.72	-6.71	0.16	-1.30	-0.74	0.49	-0.70
Ti	16.36	2.7	-6.44	1.59	-1.48	-1.21	-0.15	-0.24
V	16.35	2.69	-5.46	1.55	-0.95	-0.78	0.14	-0.64
Cr	16.33	2.69	-4.31	1.24	-0.11	0.03	1.46	0.61
Mn	16.33	2.69	-2.60	0.11	-0.22	-0.09	-1.43	-0.62
Fe	16.32	2.68	-4.90	2.00	1.15	1.28	1.23	-0.09
Co	16.31	2.67	-4.99	2.21	0.27	0.81	0.33	-0.32
Ni	16.29	2.66	-4.92	2.20	0.48	0.48	0.14	-0.16
Cu	16.29	2.67	-4.34	2.51	1.00	1.00	0.17	0.36
Zn	16.33	2.69	-2.93	0.70	0.86	0.86	1.15	0.33
Zr	16.40	2.74	-7.25	0.36	-2.23	-1.80	-0.70	-0.60
Nb	16.37	2.72	-7.17	1.29	-2.16	-2.16	-1.03	-0.80
Mo	16.35	2.71	-7.29	2.23	-0.74	-0.19	-0.22	-0.51
Ru	16.33	2.70	-5.61	3.27	-0.03	0.24	-0.61	-1.01
Rh	16.32	2.70	-5.35	3.28	0.37	0.48	-0.75	-0.42
Pd	16.32	2.70	-4.31	3.10	1.12	1.12	0.19	0.38
Ag	16.32	2.75	-3.40	4.20	1.24	1.24	1.48	0.38
Cd	16.37	2.75	-2.43	0.82	0.83	0.83	1.04	0.68
Hf	16.39	2.71	-7.60	0.35	-2.21	-1.81	-0.68	-0.41
Ta	16.37	2.70	-7.90	2.03	-2.07	-1.74	-1.01	-0.97
W	16.35	2.70	-6.23	2.18	-1.24	-0.88	-0.66	-0.89
Re	16.34	2.71	-8.83	3.24	-0.17	0.56	-0.40	-0.65
Os	16.32	2.69	-5.46	1.52	-0.55	-0.16	-1.31	-1.62
Ir	16.32	2.70	-6.01	3.16	0.32	0.32	-1.13	-0.56
Pt	16.31	2.70	-5.90	4.13	1.24	1.24	-0.28	0.35
Pristine	16.32	2.72	-4.07	2.85	1.62	1.94	0.40	0.40

Table S2. The Gibbs free energy change for NO adsorption with different configurations.

TM	G_{*NO}(O-end)	G_{*NO}(N-end)	G_{*NO} (NO-Side)
Sc	1.08	-0.52	-0.52
Ti	-0.09	-1.27	-1.10
V	-0.26	-2.02	-1.15
Cr	-0.71	-2.69	-2.69
Zr	0.41	-0.95	-0.49
Nb	-0.15	-2.05	-1.29
Mo	-0.89	-2.72	-1.74
Hf	0.25	-0.40	-0.87
Ta	-0.35	-1.24	-0.84

Table S3. The comparison of U_L and PDS between this work and previous work.

Catalyst	U_L (V)	PDS	Reference
V@goldene	-0.18	$*NO_3 \rightarrow *NO_3H$	This work
VN_3B_1	-0.28	$*NO_3 \rightarrow *NO_3H$	Chin. Chem. Lett., 2026, 11273
Ir_3Ti_1	-0.22	$*NO \rightarrow *NOH$	J. Energy Chem., 2023, 112, 84
Ag/O_v-MXene	-0.24	$*NO_2 \rightarrow *NO_2H$	Small, 2024, 20, 2306311
Cr-GY	-0.36	$*NH_2 \rightarrow *NH_3$	Mater. Today Sustain, 2024, 28, 10104
Ru-Cl-C_7N_3	-0.38	$*NO \rightarrow *NOH$	Chem. Eng. J., 2026, 534, 17535
V-N_3/BP	-0.22	$*NO_3 \rightarrow *NO_3H$	Appl. Surf. Sci., 2025,714, 16440
WPP	-0.33	$*NH_2 \rightarrow *NH_3$	Int. J. Hydrog. Energy, 2024, 80, 586
Pt-N_4/C,	-0.48	$*NO \rightarrow *NOH$	ACS Catal., 2022, 12, 5407
Ti/g-CN	-0.39	$*NO \rightarrow *NOH$	Adv. Funct. Mater., 2021, 31, 2008533

Table S4. The Gibbs free energy change for NO_3RR to NH_3 on TM@goldene under N-end mechanism.

	Ti	V	Cr	Zr	Nb	Mo	Ta
ΔG_{*NO3}	-1.48	-0.95	-0.11	-2.23	-2.16	-0.74	-2.07
ΔG_{*NO3H}	0.01	0.18	0.60	0.18	-0.21	-0.10	-0.40
ΔG_{*NO2}	-1.36	-1.65	-1.05	-1.51	-1.25	-1.47	-1.09
ΔG_{*NO2H}	0.32	0.11	-0.45	0.44	0.27	-0.19	-0.28
ΔG_{*NO}	-1.27	-2.02	-2.69	-0.95	-2.05	-2.72	-1.24
ΔG_{*NOH}	-0.34	-0.07	0.62	-0.19	-0.27	0.39	-0.47
ΔG_{*N}	0.14	-0.98	-1.63	0.33	-0.74	-1.80	-0.35
ΔG_{*NH}	-2.23	-1.02	-0.20	-2.48	-1.43	-0.33	-1.93
ΔG_{*NH2}	-0.81	-0.24	-0.70	-1.12	-0.12	0.17	-0.20
ΔG_{*NH3}	0.08	-0.20	0.02	0.18	0.61	0.23	0.89
$\Delta G_{* + NH3}$	1.31	1.19	-0.04	1.70	1.71	0.91	1.47

Table S5. The Gibbs free energy change for NO_3RR to NH_3 on TM@goldene under N-side mechanism.

Intermediate	Sc	Hf
ΔG_{*NO3}	-1.30	-2.21
ΔG_{*NO3H}	1.12	0.13
ΔG_{*NO2}	-2.45	-1.45
ΔG_{*NO2H}	0.64	0.43
ΔG_{*NO}	-0.74	-0.87
ΔG_{*NOH}	-0.80	-1.00
ΔG_{*NOH2}	-1.27	-1.05
ΔG_{*O}	-0.25	-1.13
ΔG_{*OH}	-1.74	-0.95
$\Delta G_{* + H2O}$	1.25	2.56

Table S6. The charge changes of intermediates adsorption on Ti, V, Zr, and Mo@goldene

Intermediate	Ti	V	Mo	Zr
*NO_3	0.60	0.61	0.59	0.65
*NO_3H	0.92	0.83	0.79	1.08
*NO_2	0.69	0.66	0.66	0.68
*NO_2H	0.49	0.21	0.46	0.53
*NO	0.67	0.68	0.67	0.76
*NOH	0.59	0.32	0.46	0.62
*N	0.87	0.61	0.76	0.95
*NH	0.66	0.43	0.46	0.83
*NH_2	0.31	0.29	0.18	0.40
*NH_3	-0.17	-0.16	-0.19	-0.13

Figure S1. The total density of state of pristine goldene.

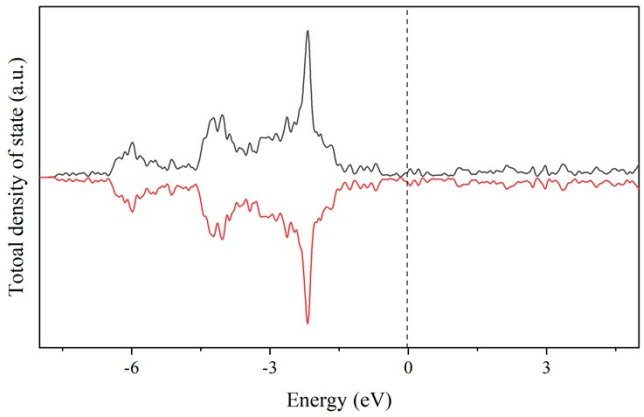

Figure S2. Pourbaix diagram of nitrogen species. X-axis: pH value (0-14), representing the acidity/basicity of the solution. Y-axis: Electrode potential (U *vs*. SHE). Higher values mean stronger oxidizing conditions; lower values mean stronger reducing conditions. Solid black lines**:** Thermodynamic equilibrium boundaries between different nitrogen species. On these lines, the species on both sides coexist in equilibrium. Blue dashed lines: The stability window of water. Upper dashed line: O_2/H_2O equilibrium. Above this line, water is oxidized to O_2. Lower dashed line: H_2O/H_2 equilibrium. Below this line, water is reduced to H_2. Most aqueous nitrogen redox reactions occur within this water-stable window. The temperature and pressure should be ambident temperature and pressure.

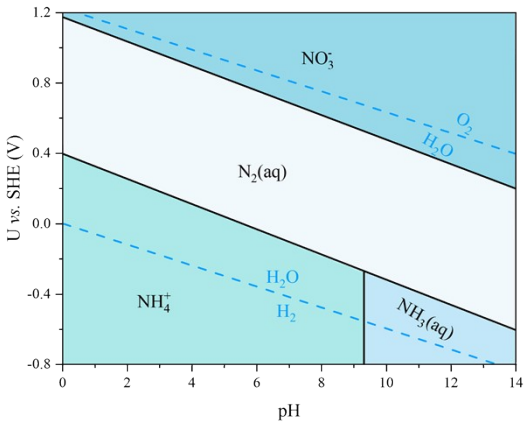

Figure S3. The Gibbs free energy change for $*NO_3$, *H, and $*N_2$ adsorption.

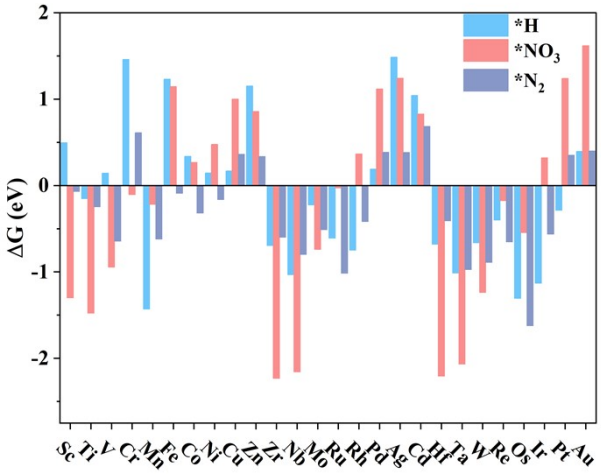

Figure S4. The Gibbs free energy change for NO_3RR to NH_3 on TM@goldene. Step 0 and 10 is the non-electrochemical step, while other numbers indicate the number of PCET steps.

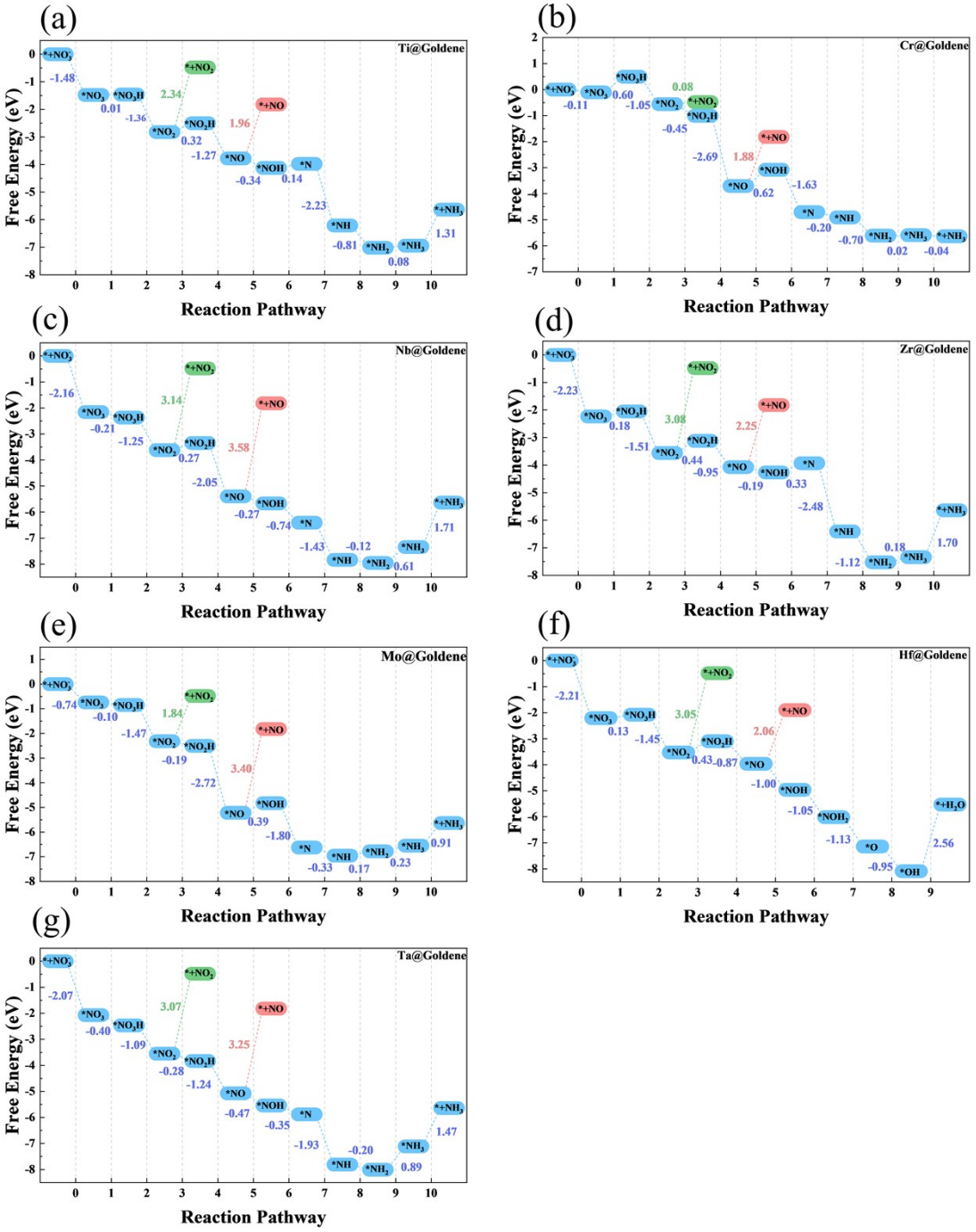

Figure S5. The energy barrier of the coupling of two NO to *N_2O_2 on (a) Ti@goldene, (b) Zr@goldene.

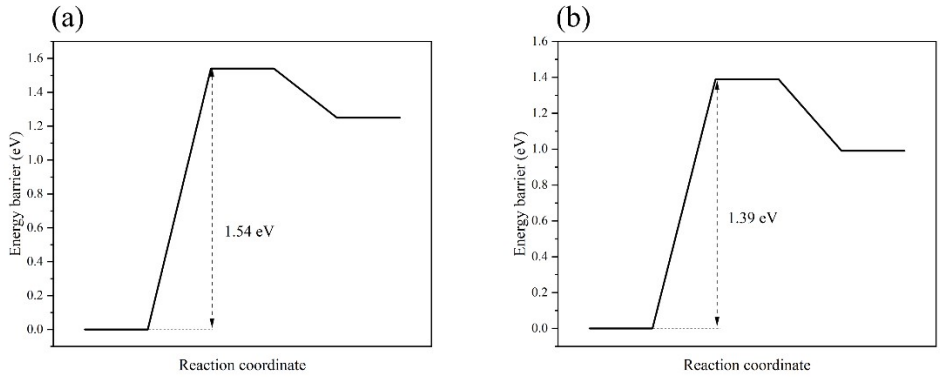

Figure S6. The totaldensity of state of (a) Ti@goldene, (b) V@goldene, (c) Zr@goldene, and (d) Mo@goldene.

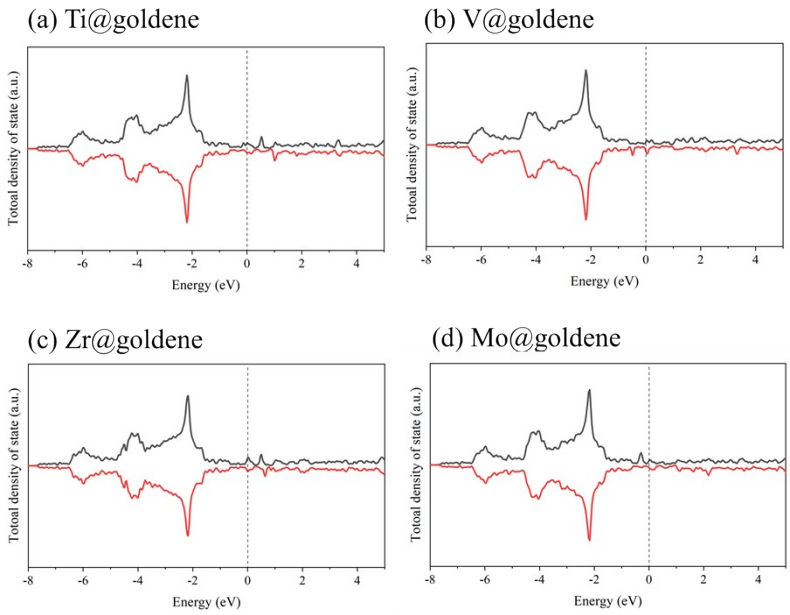

Figure S7. The AIMD of (a) Ti@goldene, (b) V@goldene, (c) Zr@goldene, and (d) Mo@goldene at 300K for 10 ps.

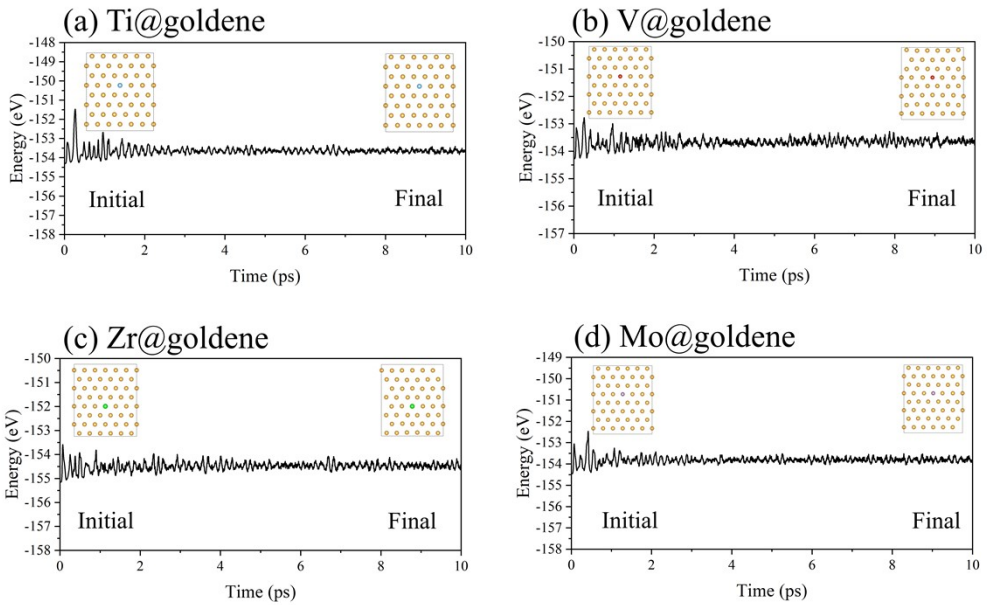

Figure S8. The Gibbs free energy change for NO3RR to NH3 on V@goldene performed by DFT+U with U = 4 eV, J = 1 eV.

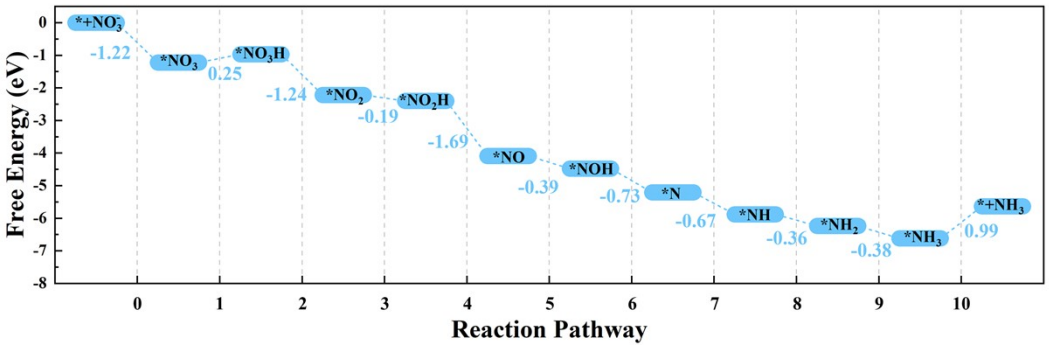

Figure S9. The partial density of state of (a)Ti@goldene, (b) V@goldene, (c) Zr@goldene, and (d) Mo@goldene

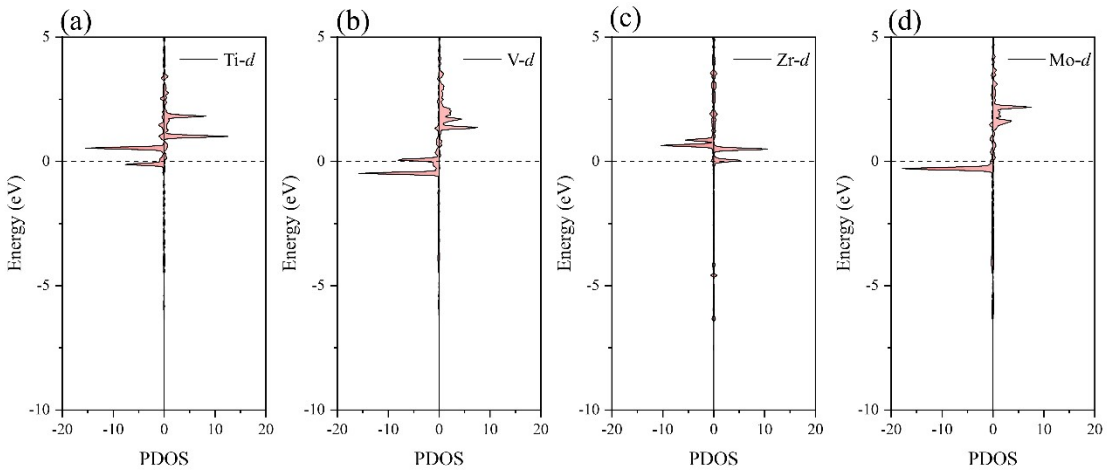

Figure S10. The relationship between d band center and ΔG for NO_3^- adsorption.

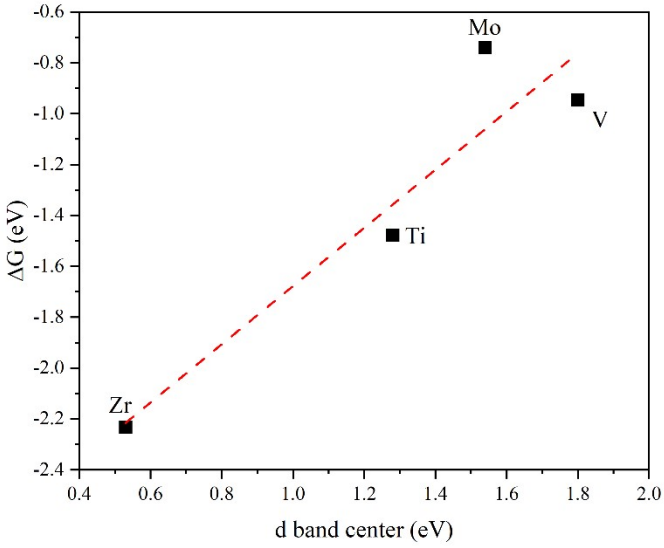

Figure S11. The partial density of state of NO_3^- adsorption on (a) Ti@goldene, (b) V@goldene, (c) Zr@goldene, and (d) Mo@goldene

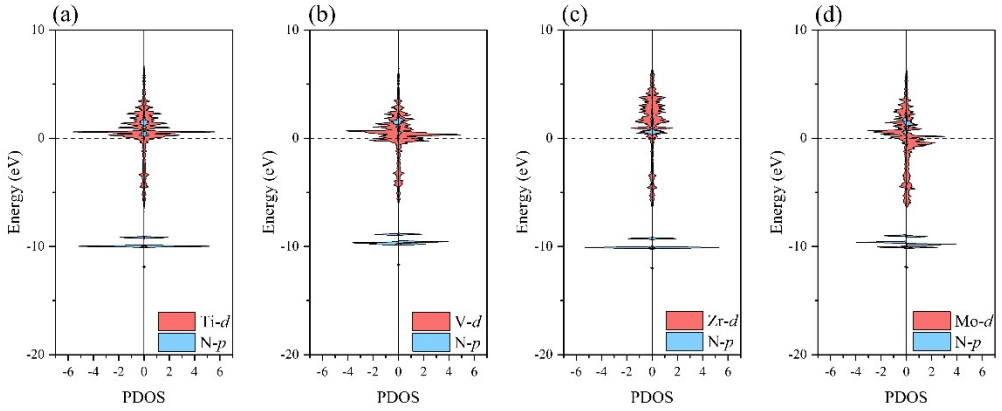

Reference

1. S. Zhu, M. Qin, L. Chen, S. Jiang, Y. Zhou, J. Jiang and W. Zhang, Theoretical investigation of electrocatalytic reduction of nitrates to ammonia on highly efficient and selective g-C_2N monolayer-supported single transition-metal atoms, *J. Phys. Chem. Lett.*, 2023, **14**, 4185-4191.
2. H. Niu, Z. Zhang, X. Wang, X. Wan, C. Shao and Y. Guo, Theoretical insights into the mechanism of selective nitrate-to-ammonia electroreduction on single-atom catalysts, *Adv. Func. Mater.*, 2020, **31**, 2008533.
3. Y. Pang, Z. Ding, A, Ma, G. Fan, H. Xu, Electroreduction of nitrate to ammonia on graphyne-based single-atom catalysts by combined density functional theory and machine learning study, Sep. Purif. Technol., 2025, **354**, 129422.